Bubble characterization and gas–liquid interfacial area in two phase gas–liquid system in bubble column at low Reynolds number and high temperature and pressure

Dan Feng, Jean-Henry Ferrasse, Audrey Soric, Olivier Boutin

Bubble characterization and gas-liquid interfacial area in two phase gas-liquid system in bubble column at low Reynolds number and high temperature and pressure

Dan Feng, Jean-Henry-Ferrasse, Audrey Soric, Olivier Boutin

Aix Marseille Univ, CNRS, Centrale Marseille, M2P2, Marseille, France

Corresponding author: Olivier Boutin olivier.boutin@univ-amu.fr

AMU M2P2 Europôle de l'Arbois BP80 13545 Aix en Provence Cedex 4, France

Abstract

Bubbles hydrodynamic in gas liquid contactor, including bubble size distribution, bubble size and gas-liquid interfacial area, was evaluated as a function of superficial gas velocity, superficial liquid velocity, temperature, pressure and different gases (N_2 and He) and liquids (water and ethanol/water mixture) phases. The results showed that with the increase of superficial gas velocity, the bubble size distribution shifted from smaller- to larger-size bubble and the Sauter mean diameter, the gas holdup and the interfacial area generally increased due to the increase of coalescence. The effect of superficial liquid velocity on bubble characteristics was not significant. Pressure and temperature showed slight influence on gas holdup and interfacial area. The bubble characteristics were not significantly influenced by the type of gas phase, but mainly affected by the liquid composition. Correlations to predict Sauter mean bubble diameter and the gas holdup are developed using Kanaris correlation and in good agreement with experimental results.

Highlights

- Study of hydrodynamics of bubble column under high pressure and temperature.
- Bubble diameter, gas holdup and interfacial area increases with superficial gas velocity.
- The type of gas phase influences bubble characteristics.
- Correlations to predict Sauter mean bubble diameter and gas holdup are developed.

Keywords: bubble column; bubble size distribution; gas holdup; interfacial area, wet air oxidation

Nomenclature

a	gas-liquid interfacial area (m^{-1})
a_1-a_5	parameter used in Eq. (6)
b_1-b_5	parameter used in Eq. (7)
Ar	Archimedes number ($= {gD^3\rho_L^2}/{\mu_L^2}$)
D	column diameter (m)
$d_{b,i}$	equivalent bubble diameter defined in Eq. (1) (m)
$d_{b,max}$	maximum bubble diameter (m)
$d_{b,min}$	minimum bubble diameter (m)
$d_{b,eq}$	equivalent mean bubble diameter (m)
$d_{b,i}$	initial bubble diameter at class i (m)
$d_{b,i+1}$	final bubble diameter at class i (m)
d_P	sparger column (m)
d_{32}	Sauter mean diameter (m)
Eo	Eötvös number ($= {gD^2\rho_L}/{\sigma_L}$)
Fr	Froude number ($= {U_G{}^2}/{gD}$)
g	gravitational constant ($m.s^{-2}$)
Mo	Morton number ($= {g\mu_L{}^4}/{\rho_L\sigma_L^3}$)
N	number of bubble classes
n_i	bubble number of each class
Oh	Ohnesorge number ($= {\mu_L}/{\sqrt{\rho_L\sigma_L D}}$)
P	Pressure (MPa)
Re	Reynolds number ($= {\rho_L U_G D}/{\mu_L}$)
S	sample size
T	Temperature (K)
U_G	gas superficial velocity ($cm.s^{-1}$)
U_L	liquid superficial velocity ($cm.s^{-1}$)
$V_{b,i}$	bubble volume at each class (m^3)
V_c	column volume (m^3)
We	Weber number ($= {\rho_L U_G^2 D}/{\sigma_L}$)

Greek letters

ε_G gas holdup (-)
μ_L liquid viscosity (kg.(m s)$^{-1}$)
ρ_L liquid density (kg.m^{-3})
σ_L liquid surface tension (N.m^{-1})

1 Introduction

Bubble columns are widely used in many industrial gas-liquid operations (*e.g.* wet air oxidation, gas/liquid reactions, fermentations, agitation by gas injection) in chemical and biochemical industries due to their simple construction, no mechanically moving parts, low operating cost, high thermal stability, high-energy efficiency and good mass transfer capabilities (Kanaris et al., 2018). Most research for bubble columns focused on ambient conditions, while many industrial bubble columns are operated at extreme conditions with high temperatures and pressures (Pohorecki et al., 2001 ; Léonard, 2015). Among the different processes operated in bubble columns, Wet Air Oxidation (WAO) is for instance widely recognized as one of the most efficient technology for wastewater treatment with high pollutant removal efficiency and less toxic by-products (Barge and Vaidya, 2018). WAO accomplishes oxidation at high temperature (up to 325□) and high pressure (up to 30MPa) (Leonard et al., 2015). To design and optimize WAO processes, it is necessary to predict the mass transfer efficiency in the bubble column. However, in the literature, almost no papers reported bubble columns studies under WAO conditions. Only few research have been carried out at temperatures over 373K or at pressure over 3MPa in air-water or oxygen-water systems (Behkish et al., 2007; Clark, 1990; Jin et al., 2014; Lau et al., 2004; Luo et al., 1999; Pohorecki et al., 2001; Wilkinson et al., 1992). Consequently, this article proposes an experimental focus on bubbles characterisation in WAO process conditions and can be obviously used in any gas liquid contactor working in these conditions.

In all above processes, bubble size distribution and gas holdup are important design parameters, which have been often used to define the gas-liquid interfacial area available for mass transfer (Akita and Yoshida, 1974; Kanaris et al., 2018; Majumder et al., 2006; Pohorecki et al., 2001; Stegeman et al., 1996). The operation of bubble columns can be affected by several parameters. Gas and liquid superficial velocities, temperature, pressure, liquid-phase viscosity, density and surface tension have been indicated to affect the formation

and stability of the gas bubbles and then the hydrodynamic and mass transfer behaviour in the bubble column reactors (Behkish et al., 2007).

Table 1 summarizes available literature studies on the influence of operation parameters on bubble characteristics in bubble columns. Many research reported that with the increase of gas superficial velocity, the gas holdup enhanced, inducing an increase in bubbles number, turbulence and collision frequency, resulting in the increase of bubble size (Behkish et al., 2007; Clark, 1990; Kanaris et al., 2018; Lau et al., 2004; Luo et al., 1999; Majumder et al., 2006; Wilkinson et al., 1992). However, Mohagheghiana and Elbing (2018) and Akita and Yoshida (1974) both observed a decrease in Sauter mean diameter of bubbles with increasing gas superficial velocity. Majumder et al. (2006) indicated that in an air-water system, bubble size decreased with increasing liquid superficial velocity, due to bubble breakup. Chaumat et al. (2005) indicated that in a cyclohexane/N_2-CO_2 system, gas holdup decreased by increasing the liquid superficial velocity. For an air-water system, Schäfer et al. (2002) reported a significant decrease of bubble size when increasing the pressure up to 5MPa at ambient temperature with different types of spargers in the homogeneous regime, while a plateau for the effect of pressure on bubble size has been observed by some authors (Chilekar, 2007; Chilekar et al., 2010; Hashemi et al., 2009; Kumar et al., 2012; Pjontek et al., 2014). Moreover, it is commonly observed by many authors that a pressure increase results in an increase of gas holdup (Chilekar et al., 2010; Hashemi et al., 2009; Kumar et al., 2012; Maalej et al., 2003; Pjontek et al., 2014; Therning and Rasmuson, 2001; Urseanu et al., 2003), which is attributed to the increase of gas density, the reduction of the bubble size, and the increase of bubble number density (Behkish et al., 2007). Generally, with the increase of temperature, bubble diameter decreases and gas holdup increases (Behkish et al., 2007; Hashemi et al., 2009; Lau et al., 2004), while no effect (Pohorecki et al., 1999) or even negative effect (Deckwer et al., 1980; Grover et al., 1986; Yang et al., 2001) of temperature on gas holdup have been reported. Lin et al. (1998) reported a decrease of the maximum stable bubble size of N_2 in Paratherm NF fluid with temperature due to a combined effect of the decrease of surface tension and liquid viscosity. Several publications also revealed that gas holdup increased with the reduction of liquid viscosity and surface tension (Kawase et al., 1992; Wilkinson et al., 1992). Apart from pressure and temperature, physical properties of the phases can also play a role in the bubble characteristics. This influence will be tested using different gases and liquids, allowing significant variations of the phases properties.

For the design and scale-up of bubble column reactors for industrial processes, the knowledge of mass transfer between gas-liquid contacting systems is required. In many gas-liquid systems, the mass transfer rate is controlled by volumetric mass transfer coefficient, which is a function of specific interfacial area (Majumder et al., 2006). Thus, it is essential to study the interfacial phenomena in the gas-liquid system at different operating conditions. In recent years, most research focused on mass transfer characteristics in bubble columns at atmospheric conditions, few data obtained on volumetric mass transfer coefficient and interfacial area at high pressure and high temperature (Jin et al., 2014). Pohorecki et al. (1999) and Baz-Rodríguez et al. (2014) reported that with the increase of the superficial gas velocity, the interfacial area increased. Chaumat et al. (2005) found that the local interfacial area decreased with superficial liquid velocity in different liquid-gas phase with cyclohexane or water as liquid phase and N_2 or CO_2 as gas phase. Oyevaar and Westerterp (1991) observed a positive influence of pressure on the interfacial areas at pressure up to 8MPa in a mechanically stirred gas-liquid reactor and a bubble column, consistent with Stegeman et al. (1996) . Sehabiague et al. (2005) reported that volumetric mass transfer coefficient values and gas holdup increased with the increase of the pressure, operating temperature and superficial gas velocity in a slurry bubble column under the range of pressure 0.17-3.0MPa and the range of temperature 298-453K. However, at low superficial gas velocity (U_G < 3cm.s^{-1}), no effect of pressure on mass transfer was observed for pressure between 0.1-0.8MPa (Wilkinson et al., 1994) and a decrease of the values with pressure was reported by Maalej et al. (2003). Furthermore, most research point out that the interfacial area values seems to increase with the increase of temperature (Jin et al., 2014; Pohorecki et al., 2001). Nevertheless, it was also reported that the interfacial area increased with increasing superficial gas velocity and pressure, while decreased with the increase of the temperature (Lau et al., 2004). All this literature analysis is summed up in Table 1.

Table 1 Available literature studies on bubble characteristics in bubble column reactors

Authors	System	Conditions	Remarks
(Akita and Yoshida, 1973)	D=0.15m, H=4m Air-H_2O, glycol, carbon tetrachloride, methanol	P: 0.1MPa; T: 293K; U_G: up to 0.33m.s^{-1}	d_{32} decreased with U_G
(Clark, 1990)	D=0.075m, H=3m N_2, H_2-H_2O, CH_3OH	P:2.5-10MPa; T: 293-453 K; U_G: 0.002-0.055m.s^{-1}; U_L:0.0014m.s^{-1}	ε_G increased with U_G and P
(Oyevaar et al., 1991)	D=0.081 m, H=0.081 and 0.81 m N_2, CO_2-water, diethanolamine	P: 1-8.0 MPa; T: 298 K U_G: 0.01-0.1 m/s	ε_G increased with P; the increase of a with increasing P was larger for higher U_G;
(Wilkinson et al., 1992)	D=0.158m, H=1.5m N_2-H_2O, n-Heptane, Mono-ethylene glycol	P: 0.1-2.0MPa; T: 293-313K; U_G: 0.002-0.055m.s^{-1}; U_L: 0.11m.s^{-1}	ε_G increased with U_G and P
(Wilkinson et al., 1994)	D=0.158 m, H=1.5 m He, N_2, Ar, CO_2, SF_6-water, n-Heptane, Mono-ethylene glycol, Na_2SO_3	P: 0.1-0.8 MPa; T: 293 K; U_G: up to 0.2 m/s	ε_G increased with P; volumetric mass transfer coefficient increased with P at high U_G; while no effect of P at low U_G
(Stegeman et al., 1996)	D=0.156 m, H=0.64 m N_2, CO_2-water, diethanolamine	P: 0.1-6.6 MPa; T: 298 K U_G: up to 0.06 m/s	ε_G increased with U_G; a increased with P and moderately affected by U_G
(Lin et al., 1998)	D=0.0508-0.1016 m, H=0.8-1.58 m N_2-Paratherm NF	P: up to 20 MPa; T: 300-351 K; U_G: 0.02-0.08 m/s	ε_G increased with P and T; Maximum stable bubble size decreased with T and P
(Luo et al., 1999)	D=0.102m, H=1.37m N_2-Paratherm NF	P: 0.1-5.6MPa; T: 301 and 351K; U_G: up to 0.4m.s^{-1}	ε_G increased with U_G and P; Smaller bubble size at high pressure; Maximum bubble size increased with U_G, but decreased with P
(Pohorecki et al., 1999)	D=0.304 m, H=3.99 m N_2-H_2O	P: 0.1-1.1 MPa; T: 303-433℃; U_G: 0.002-0.055	d_{32} slightly with U_G; No influence of P and T on d_{32} and ε_G

		m/s; U_L: up to 0.02 m/s	
(Pohorecki et al., 2001)	D=0.3 m, H=4 m N_2-cyclohexane	P: 0.2-1.1 MPa; T: 303-433 K; U_G: 0.002-0.055 m/s; U_L: 0.14 cm/s	No effect of P and T on d_{32}; no effect of P on ε_G; ε_G increased with T; a increased with T
(Schäfer et al., 2002)	D=0.54 m, H=0.475 m N_2-H_2O, cyclohexane, Na_2SO_4 solution	P: up to 5 MPa; T: up to 448 K; U_G: up to 0.37 cm/s	d_{32} decreased with P; d_{32} increased along the height of column; Effect of T on d_{32}
(Maalej et al., 2003)	D=0.046 m, H=0.25 m N_2, CO_2-NaOH, Na_2CO_3/NaHCO3	P: up to 5 MPa; T:293 K; U_G: up to 0.03 m/s; U_L:0.067 m/s	a increased with P
(Lau et al., 2004)	D=0.0508m and 0.1016m N_2, air-Paratherm NF	P: up to 4.24MPa; T: up to 365K; U_G: up to 0.4m.s^{-1}; U_L: 0.08-0.89cm.s^{-1}	ε_G increased with U_G, T and P, but slightly decreased with U_L; a increased with P and T;
(Chaumat et al., 2005)	D=0.2m, H=1.6m N_2, CO_2-H_2O, cyclohexane	P: atmospheric pressure; T: 293K; U_G: up to 0.14m.s^{-1}; U_L: up to 0.08m.s^{-1}	ε_G increased with U_G, but slightly decreased with U_L; ε_G was slightly greater in cyclohexane than in H_2O
(Sehabiague et al., 2005)	D=0.3 m, H3 m N_2, He-Fishcher-Tropsch	P: 0.17-3.0 MPa; T: 298-453 K	ε_G and mass transfer parameters increased with U_G, P and T
(Majumder et al., 2006)	D=0.05m, H=1.6m Air-H_2O	P: atmospheric pressure; T: 302K; U_G: 0.17-1.358cm.s^{-1}; U_L: 7.07-14.14cm.s^{-1}	d_{32} increased with U_G, but decreased with U_L; a increased with U_L
(Behkish et al., 2007)	D=0.29m, H=3m N_2, He-Isopar-M	P: 0.67-3MPa; T: 300-473K; U_G: 0.07-0.39m.s^{-1}	ε_G increased with U_G, and T; Effect of P on ε_G; d_{32} decreased with P; Effect of T on d_{32}; d_{32} (N_2)> d_{32} (He)
.(Baz-Rodríguez et al., 2014)	D=0.095 m, H=1.2 m O_2-H_2O, NaCl, $MgCl_2$, $CaCl_2$	P: atomospheric pressure; T: 303 K; U_G: 0.0005-0.0197 m/s	a increased with U_G;
(Jin et al., 2014)	D=0.1m, H=1.25m H_2, CO, CO_2-Paraffin	P: 1.0-3.0MPa; T: 293-473K; U_G: 0.03-0.1m.s^{-1}	a increased with U_G, P and T
(Kanaris et al., 2018)	D=0.05m, H=0.35m Air, CO_2, He-H_2O, aqueous glycerine (40%, v/v)	P: atmospheric pressure; T: ambient temperature; U_G: 0-0.064m.s^{-1}	ε_G increased with U_G; d_{32} was not considerably affected by gas type but mainly affected by liquid type

(Mohagheghian and Elbing, 2018)	D=0.063-0.102m, H=0.61-1.22m Air-H_2O	P: up to 0.6MPa; T: 293 -295K; U_G: 0.14-5.5cm.s^{-1}; U_L: up to 0.08	d_{32} decreased with U_G

Therefore, the objective of this study is to investigate the effect of gas and liquid superficial velocity, pressure (10-20MPa), temperature (373-473K) on bubble size distribution and interfacial area. In order to evaluate these effects in very different conditions, the physical properties of the phases must be changed on a large range. For that purpose, different liquid-gas systems (water-N_2 system, water-He system, ethanol/water mixture-N_2 system and ethanol/water mixture-He system) has been used.

2 Experimental methods

2.1 Experimental setup

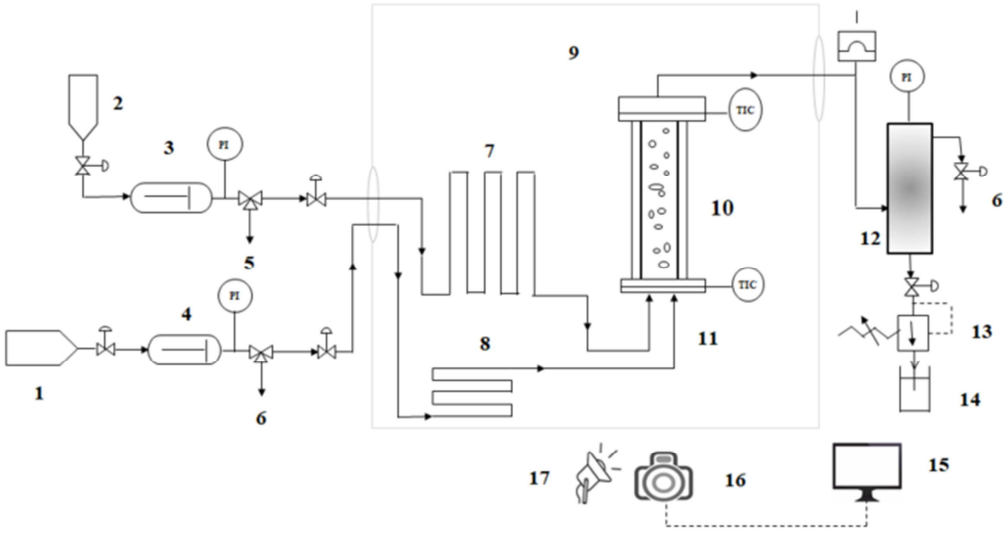

Fig. 1 Schematic diagram of experimental setup. 1 – gas tank; 2 – syringe used for liquid; 3 – liquid pump; 4 – gas pump; 5 – liquid purge; 6 – gas purge; 7 – liquid coil; 8 – gas coil; 9 – oven; 10 – bubble column; 11 – gas sparger; 12 – buffer tank; 13 – pressure limiter; 14 – liquid outlet; 15 – monitor; 16 – camera; 17 – lamp.

Fig. 1 shows a schematic diagram of the bubble column used in this study (Top Industrie, France). The system consists of a vertical column, liquid and gas supplying equipment, two piston pumps used for gas and liquid, a liquid exhaust reservoir, an oven, a buffer tank and a pressure limiter. The bubble column, made of sapphire, has an internal diameter of 1cm and an outer diameter of 2.4cm with 0.7cm thick wall. The height and the total volume of the bubble column are 10cm and 8mL, respectively. The column is intended to operate at pressures up to 20MPa and temperatures up to 473K. The liquid pump is a volumetric piston pump, with a total volume of 53mL, delivering a liquid flowrate up to 16 $mL.min^{-1}$. In this study, the liquid flow rate was set at 1, 3 and 5 $mL.min^{-1}$ (i.e. liquid superficial velocity of

0.022, 0.066 and 0.122 $cm.s^{-1}$ respectively). These values are coherent with those used in industrial bubble columns and allow enough time to reach the steady state regarding the volume of the pump reservoir. The precision on the flow rate is 0.3%. The purity of N_2 and He are both higher than 99% (supplied by Air Liquid). The gas pump is also a volumetric piston pump with total volume of 52mL and maximum flow rate of $22mL.min^{-1}$. In this study, 1-10$mL.min^{-1}$of gas flow rate was used to obtain gas superficial velocity of 0.028-0.276$cm.s^{-1}$. The gas phase is injected through a nozzle with an average pore size of 80μm. The temperature of both fluids is controlled in the oven, a vitreous oven with a volume of 32 L (Memmert). The temperature of the oven is controlled up to ±0.1□. A pressure limiter (TESCOM) is used for pressure regulation, controlled by the user through a pressure sensor. A buffer tank is placed before pressure reduction to avoid large rises or declines of pressure or non-negligible pressure oscillations in the bubble column during the passage from the liquid to the gas through the pressure limiter. A camera is used to record the bubbles behaviour in the column with a 19MPixel resolution, equipped with a 69mm macro lens with fixed focal length (Canon EOS M®). The accuracy of diameter measurement with a photo is ±38μm (corresponding to 2 Pixels).

In this study, N_2 or He and water or ethanol/water mixture are used as the gas and liquid phase respectively. The operating variables are shown in Table 2. With the increase of pressure, the density of gas phase significantly increases, while the effect on liquid properties, gas viscosity and dimensionless numbers are independent. As temperature increases, gas and liquid density, liquid viscosity, liquid surface tension, *Oh* number and *Mo* number all decrease, whereas *Ar* and *Eo* number increase.

Table 2. Physical properties of liquid and gas phases at different pressures and temperatures ("Thermophysical properties of fluid systems," n.d.)

Conditions				Liquid phase			Gas phase		Dimensionless number			
Liquid phase	Gas phase	*T* (K)	*P* (MPa)	Density ($g.mL^{-1}$)	Viscosity (μPa.s)	Surface tension ($mN.m^{-1}$)	Density ($g.mL^{-1}$)	Viscosity (μPa.s)	*Ar*	*Eo*	*Mo*	*Oh*
H_2O	N_2	373	10	0.963	284.4	58.9	0.087	22.6	31978	16	3.3E-11	3.8E-4
			15	0.965	285.7	58.9	0.128	23.5	31960	16	3.3E-11	3.8E-4
			20	0.967	287.1	58.9	0.166	24.6	31943	16	3.4E-11	3.8E-4
H_2O	N_2	423	10	0.922	184.9	48.7	0.077	24.4	45096	18	1.1E-11	2.8E-4
			15	0.925	186.1	48.7	0.112	25.2	45087	19	1.1E-11	2.8E-4
			20	0.928	187.3	48.7	0.145	26.0	45082	19	1.1E-11	2.8E-4
H_2O	N_2	473	10	0.871	136.4	377	0.068	26.2	54539	23	7.3E-12	2.4E-4
			15	0.875	137.6	37.7	0.100	26.8	54561	23	7.5E-12	2.4E-4
			20	0.877	138.8	37.7	0.130	27.5	54341	23	7.8E-12	2.4E-4
H_2O	He	373	10	0.963	284.4	58.9	0.012	23.2	31978	16	3.3E-11	3.4E-4
Ethanol/water mixture (1:1, v/v)	N_2	373	10	0.796	448.0	31.3	0.087	22.6	13869	24	1.6E-09	9.0E-4
	He						0.012	23.4	13869	24	1.6E-09	9.0E-4

2.2 Data analysis

2.2.1 Bubble size determination

In this study, bubble size distribution of the liquid-gas mixture was obtained by photographic method. The shapes of the bubbles were considered ellipsoidal. Under these conditions, the maximum and minimum axis of the ellipse were measured. Then an equivalent spherical bubble diameter was calculated by the following equation (Majumder et al., 2006):

$$d_{b,i} = \sqrt[3]{d_{b,max}^2 d_{b,min}} \tag{1}$$

where $d_{b,max}$ and $d_{b,min}$ are the maximum and minimum diameter of bubbles. The bubble size distributions were obtained by sorting the equivalent diameters of the bubbles into different uniform classes. The minimum number of bubble diameter classes required for the construction of the size distribution, *N*, was calculated using Sturges' rule (Sturges, 1926) given by:

$$N = 1 + \log_2 S \tag{2}$$

S is the sample size. In this study, the number of classes used for the construction of the bubble distributions is 10, with equal intervals. Furthermore, the column is divided into three vertical stages (0-3.3, 3.3-6.6 and 6.6-10cm) to evaluate the effect of the height along the column on the bubble sizes. For the consistency of the experiments, measurements of all bubbles in the column were performed with several pictures for each operating condition. Then the Sauter mean diameter (d_{32}) was calculated as follows (eq. 3):

$$d_{32} = \frac{\sum_i^N n_i d_{b,i}^3}{\sum_i^N n_i d_{b,i}^2} \tag{3}$$

where n_i is the bubble number for each class.

2.2.2 Gas holdup measurement

Gas holdup in a bubble column is defined as the fraction of the gas phase volume occupied in the total volume of two- or three-phases mixture (Tang and Heindel, 2006).

$$\varepsilon_G = \frac{\sum n_i V_{b,i}}{V_c} \tag{4}$$

$$V_{b,i} = \frac{4}{3}\pi \left(\frac{d_{b,eq}}{2}\right)^3 \tag{5}$$

$$d_{b,eq} = \frac{d_i + d_{i+1}}{2} \quad (6)$$

where $V_{b,i}$ and V_c are the bubbles volume at each class and the volume of the column, respectively; $d_{b,eq}$ is the equivalent mean diameter at each class; d_i and d_{i+1} are initial diameter and final diameter at class *i*.

2.2.3 Calculation of gas-liquid interfacial area

Gas-liquid interfacial area (a) was calculated using the Sauter diameter by following equation (eq. 7) (Maceiras et al., 2010):

$$a = \frac{6\varepsilon_G}{d_{32}(1-\varepsilon_G)} \quad (7)$$

3 Results and discussion

The dominant parameter controlling bubbles dispersion state is the dynamic size variation of the bubbles due to the local bubble coalescence and breakup. It is however difficult to make an accurate evaluation of this two phenomena. Therefore, global variation of bubble size has been evaluated. Bubbles' characteristics (bubble size, gas holdup and interfacial area) are evaluated through the direct video visualization of bubbles under three pressure and temperature and different gas and liquid superficial velocity conditions. Three examples are shown in Fig. 2.

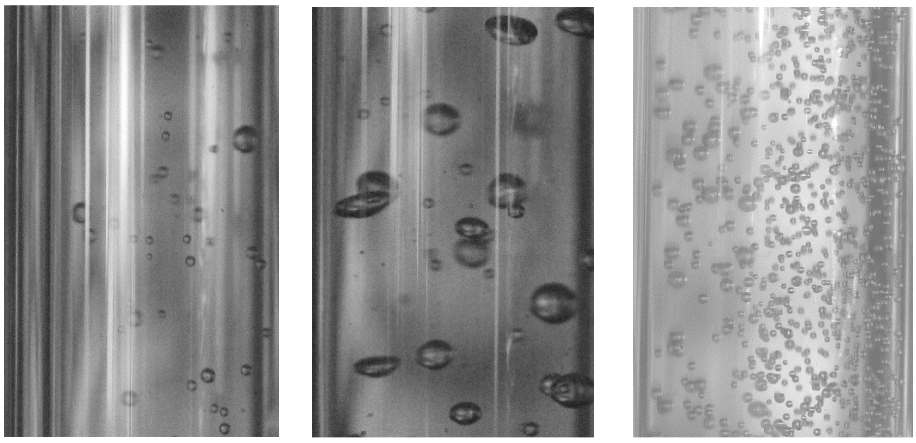

(a) (b) (c)

Fig.2 Photograph (a) N_2-H_2O system, U_G=0.083 $cm.s^{-1}$, U_L=0.022 $cm.s^{-1}$, T=373K, P=10MPa; (b) N_2-H_2O system, U_G=0.276 $cm.s^{-1}$, U_L=0.022 $cm.s^{-1}$, T=373K, P=10MPa; (c) N_2-ethanol/water mixture system, U_G=0.083 $cm.s^{-1}$, U_L=0.022 $cm.s^{-1}$, T=373K, P=10MPa

3.1 Effect of superficial gas velocity

As an example of raw data, the bubble number distribution and number fraction distribution under various superficial gas velocity and pressure at the temperature of 373K and the superficial liquid velocity of 0.022cm.s^{-1} is presented in Fig.3. The width of the distribution increases with the increase of the superficial gas velocity, which is in good agreement with the previous studies (Lin et al., 1998; Mouza et al., 2005; Ramezani et al., 2012). The trends can be due to the increase of coalescence and breakup by the increase of superficial gas velocity, resulting in the growth of collision frequency (Ramezani et al., 2012). The bubble number fraction distribution under all conditions follows the same lognormal distribution trend. At 373K and 10MPa, the bubble size distribution shifts from smaller- to larger-size bubbles and the dominant bubble size shifts from 0.45 to 0.75mm, with the increase of superficial gas velocity.

Fig.4 shows the effect of superficial gas velocity on bubble average diameter, gas holdup and interfacial area. With the increase of superficial gas velocity, the Sauter mean bubble diameter and gas holdup increase. In Fig. 2, the bubble diameter at U_G=0.276cm.s^{-1} is higher than at U_G=0.083cm.s^{-1}. This is in agreement with previous results (Hashemi et al., 2009; Li et al., 2018; Pjontek et al., 2014). This may be due to the superficial gas velocity increase, leading to more bubbles formation and the increase of the rate of coalescence, and the formation of bigger bubbles. The larger bubbles rise faster than smaller bubbles, thus the liquid resistance decreases, leading to the increase of average bubble size and gas holdup. Nevertheless, an opposite trend was also observed by other authors (Pohorecki et al., 2001; Shahrouz Mohagheghian and Brian Elbing, 2018), due to the complex role of superficial gas velocity on modifying bubble formation processes and liquid circulation (Mohagheghian and Elbing, 2018).

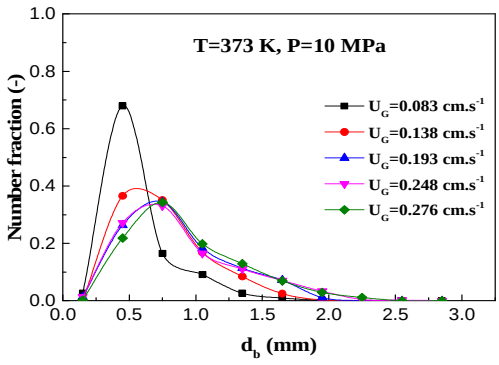

Fig. 3 Bubble number distribution and number fraction under various superficial gas velocity and at T=373K, P=10MPa and U_L =0.022cm.s^{-1}

The interfacial area calculated by Eq. (7) is shown in Fig. 4, which is related to the Sauter mean diameter and the liquid volume. It shows that the interfacial area is generally observed to be higher at higher superficial gas velocity. The similar observation has been reported by Jin et al. (2014). This can be attributed to the increase of the bubble passage frequency and gas holdup with superficial gas velocity. The mean Sauter diameters are also obtained in three axial locations (0-3.3, 3.3-6.6 and 6.6-10cm) from the bottom of the column (Fig. 5).

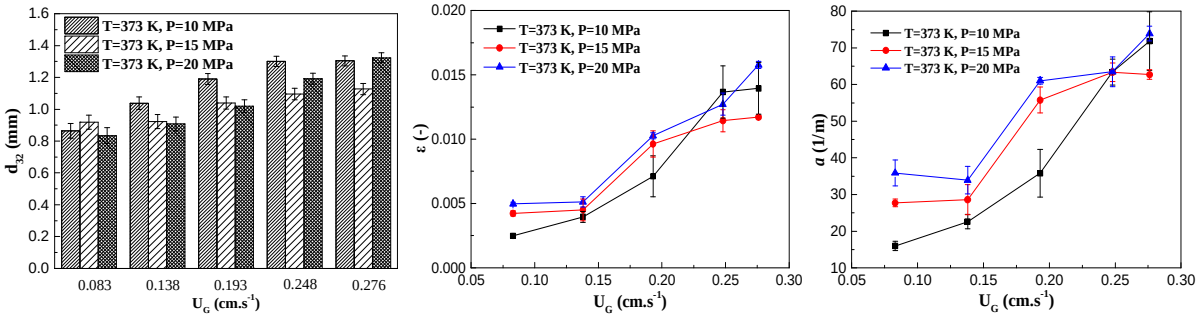

Fig. 4 Bubble mean Sauter diameter (left), gas holdup (middle) and interfacial area (right) under various superficial gas velocity and pressure at T=373K and U_L =0.022cm.s^{-1}

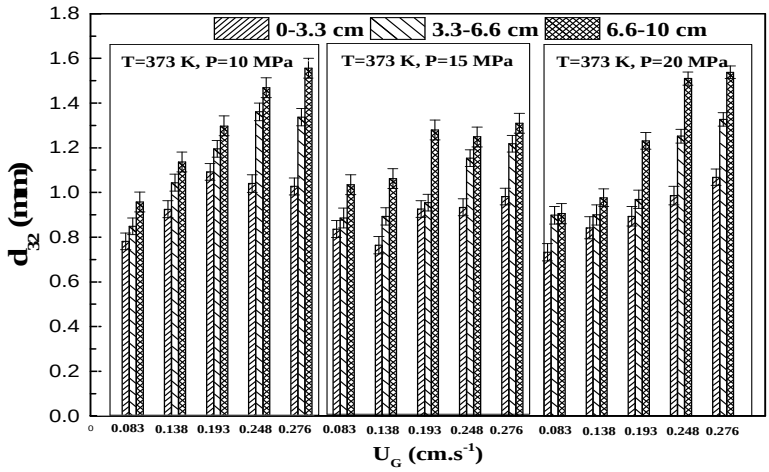

Fig. 5 Bubble mean Sauter diameter along the location of the column under various superficial gas velocity and pressure at T=373K and U_L =0.022cm.s^{-1}

The mean Sauter diameter increases with the increase distance from the bottom of the column due to the coalescence of smallest bubbles, which is in good agreement with the results reported by Majumder et al. (2006). This trend is due to the coalesced bubbles went up due to their buoyancy and accumulated along the column from the bottom to the top (Majumder et al., 2006), which is presented on Fig. 6. For each gas superficial velocity, the bubble number decreases along the height from the bottom to the top of the column, indicating the increase of coalescence. However, Pohorecki et al. (2001) observed no changes of Sauter mean diameter along the column axis in the N_2-cyclohexane system, which was attributed to the dynamic equilibrium between coalescence and redispersion processes in the column. Luo et al. (1999) revealed that the effect of the column height was insignificant for the column height above 1-3m and the ratio of the column height to the diameter larger than 5.

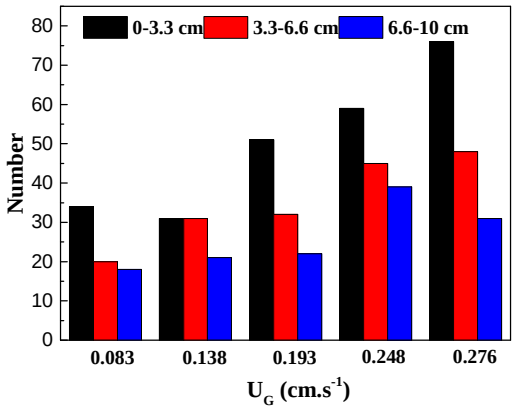

Fig. 6 Bubble number distribution along the location of the column under various superficial gas velocity at T=373K and *P*=10MPa

3.2 Effect of superficial liquid velocity

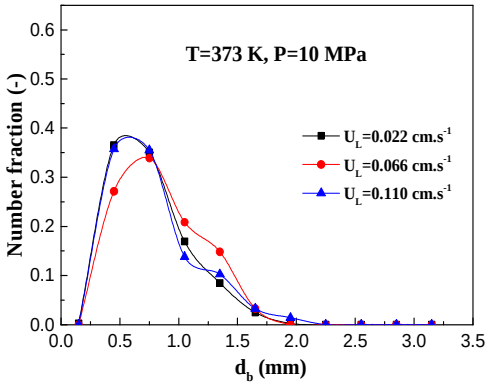

Fig. 7 Bubble number distribution and number fraction under various superficial liquid velocity at P=10MPa, T=373K and U_G =0.138cm.s^{-1}

The effects of superficial liquid velocity on bubble hydrodynamic in the column are shown in Fig. 7 and Fig. 8. Fig. 7 shows that with the superficial liquid velocity enhancement, the total bubble number little increases, and the influence of superficial liquid velocity on bubble size distribution is insignificant. Moreover, as shown in Fig. 8, the effect of superficial liquid velocity on the bubble average diameter is not significant. This figure also shows that under the temperature range 373K-423K, superficial liquid velocity displays insignificant effect on gas holdup and interfacial area, indicating that under low superficial liquid velocity conditions (superficial liquid velocity less than 1cm.s^{-1}), the liquid-phase motion has little effect on bubble characteristics. This trend is consistent with previous literature results (Akita and Yoshida, 1974; Wilkinson et al., 1992). Higher superficial liquid velocity increases the kinetic energy, the turbulence intensity, bubble-bubble interaction and bubble velocity, which reduces gas holdup (Lau et al., 2004). However, the increase of superficial liquid velocity raises bubble breakup at the distributor and thus increases gas holdup attributed to higher bubble residence times in the column (Pjontek et al., 2014). Thus, the slight increase in gas holdup is dominated by the effect of superficial liquid velocity on bubble residence time. Shah et al. (2012) has indicated that the gas holdup is more affected by the superficial gas velocity rather than the liquid velocity. Furthermore, the interfacial area increases with the increase of superficial liquid velocity, while the variation of interfacial area is small due to the marginal effect of the superficial liquid velocity on the gas holdup and bubble size for the range studied. Lau et al. (2004) observed a similar observation in the air-Paratherm system under lower pressures (up to 4.24MPa) and lower temperatures (up to 365K) with the superficial gas and liquid velocity varying up to 40 and 0.89cm.s^{-1}. While under the temperature of 473K, gas holdup and interfacial area increases with superficial liquid velocity. The reason for this trend needs to be further studied.

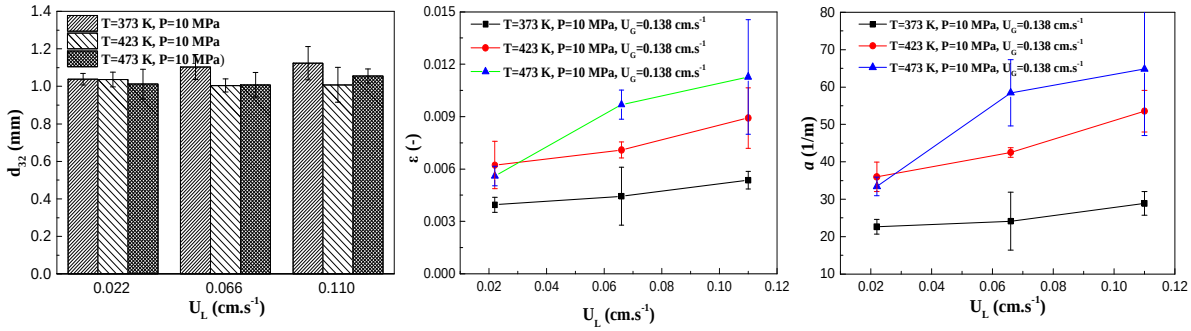

Fig. 8 Bubble mean Sauter diameter (left), gas holdup (middle) and interfacial area (right) under various superficial liquid velocity and temperature at P=10MPa and U_G =0.138cm.s^{-1}

3.3 Effect of pressure

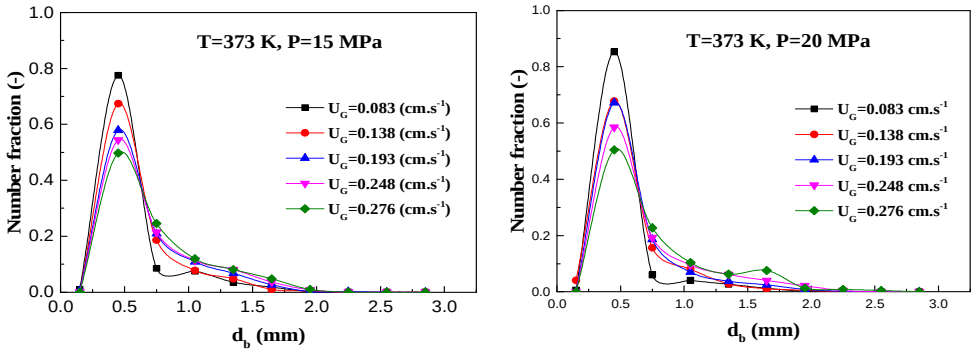

Fig. 9 Bubble number distribution and number fraction under different pressure at T=373K and U_L =0.022cm.s^{-1}

Fig. 3 and Fig. 9 demonstrate the effects of pressure on bubble size distribution at 373K. Fig. 3 and Fig. 9 show that with the increase of pressure, the bubble number increases and the bubble-size distribution shifts from large to smaller size distribution. Similar results were observed by other researchers (Lin et al., 1998). When the pressure increased from 10 to 20MPa, the dominant bubble size shifts from 0.75 to 0.45mm.

The effect of pressure on bubble average diameter is complex, but generally, with the pressure ranging from 10 to 15MPa, most of bubble mean diameters decrease (Fig. 4). The increase of pressure results in an increase in bubble breakage due to the increase of gas density with pressure, caused by the larger gas inertia in the fluctuating bubble. Fig. 10 shows that the bubble number along the location of the column always increases with the pressure, indicating the increase in bubble breakage. Increased pressure enhances the momentum of the gas jets, enforcing turbulence and decreasing initial bubble size and maximum stable bubble size (Schäfer et al., 2002). Moreover, the effect of pressure on surface tension is not significant and hence surface tension has an almost negligible influence on bubble coalescence (Schäfer et al., 2002). Thus, the mean bubble size decreases with increasing pressure from 10 to 15MPa. Nevertheless, with the pressure further increased to 20MPa, the

pressure effect on the Sauter mean diameter is more noticeable at high gas velocity ($\geq$0.248cm.s^{-1}) and slightly effect at low gas velocity. This similar phenomenon was observed by other research (Lau et al., 2004) in the air-Paratherm system with the pressure up to 4.24MPa. The more pronounced effect of the pressure at high gas velocities is may be due to the stronger bubble coalescence at high gas velocities.

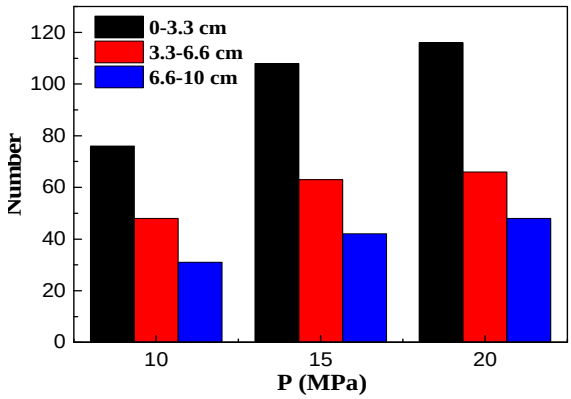

Fig. 10 Bubble number distribution along the location of the column under three pressures at T=373 K, U_G=0.276cm.s^{-1} and U_L=0.022cm.s^{-1}

Fig. 4 also shows that the gas holdup is almost independent of pressure in the studied range. Behkish et al. (2007) also reported that under high pressure from 1.7 to 3MPa, the increase of gas holdup for He and N_2 in Isopar-M/Alumina system were both insignificant. However, at the pressure below 1.7MPa, the gas holdup increased with the pressure. Under low pressure, large-size and less-dense bubbles are formed and the gas momentum enhances, which increases the rate of bubbles rupture, resulting in the increase of the gas holdup of small gas bubbles. Moreover, the increase in gas density with pressure increases the kinetic energy, leading to the increase of the collision energy which promotes the bubbles rupture (Inga and Morsi, 1999). Whereas under high pressure, the small-size and dense bubbles exists and the increasing gas momentum are not enough to rupture the small and dense gas bubbles, thus the increase of gas holdup becomes insignificant (Behkish et al., 2007). Inga and Morsi (1999) also observed the similar results: gas holdup increased under low pressures and gradually levelled off under high pressure, attributed to the balance between coalescence and the gas bubbles rupture. As shown in Fig. 4, interfacial area generally increases with the pressure ranging from 10 to 20MPa. This increasing trends is partly attributed to the relative extent to which the gas holdup slightly increases with increasing pressure and partly attributed to the reduction in bubble size with the increase of the pressure (Wilkinson et al., 1991).

3.4 Effect of temperature

Fig. 7, Fig. 8 and Fig. 11 show the effects of temperature on bubble hydrodynamics. As shown in Fig. 7 and Fig. 11, with the increase of temperature, the bubble number increases and the bubble size distribution shifts from larger- to smaller size distribution. Fig. 8 shows a little decrease on bubble average diameter with the increase of temperature, while the effect is insignificant, like the observation by Pohorecki et al. (2001). For set pressure and superficial gas velocity, gas holdup presents a small increase with increasing temperature. This general trend is due to the dominant role of associated reduction in surface tension and liquid viscosity, leading to a smaller average bubble diameter and a narrower bubble size distribution. With the decrease of liquid surface tension with temperature, the cohesive forces for maintaining gas bubbles in a spherical shape reduces and subsequently the increase of the gas momentum, leading to the rupture of large gas bubbles into smaller bubbles, hence the gas holdup increases (Behkish et al., 2007). Increasing temperature can decrease gas density, which increases the bubble size and decreases gas holdup. Furthermore, it has been reported that with the decrease of liquid viscosity, the bubble rise velocity increased, which led to a reduction of bubble residence time and subsequently reduced the gas holdup (Deng et al., 2010). As reported by Pohorecki et al. (2001), the influence of the surface tension on the gas holdup was considerably higher than that of the liquid viscosity. In this study, all the values of *Oh* number, which relates the viscous forces to inertial and surface tension forces, are small (less than 1), indicating a higher influence of the surface tension than viscosity. Therefore, the small gas holdup increases when increasing temperature is probably mainly due to the influence of the surface tension (Leonard et al., 2018). The data in Fig. 8 also shows that as the temperature ranges from 373 to 473K, the interfacial area generally increases due to the slight decrease of bubble size and the increase of gas holdup.

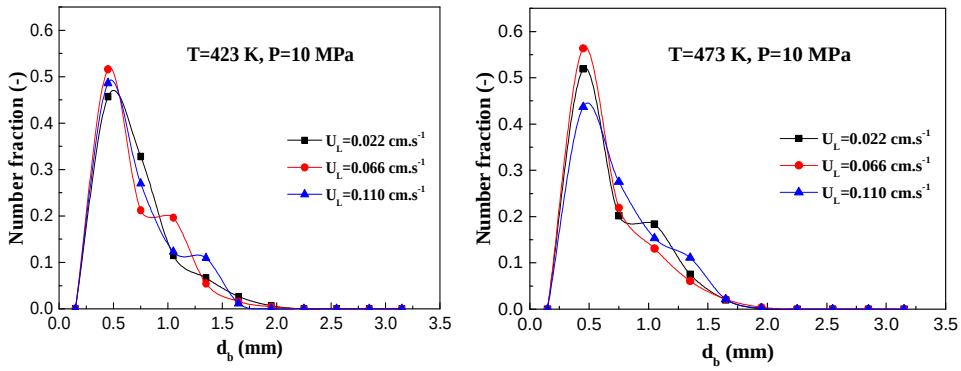

Fig. 11 Bubble number distribution and number fraction under different temperature at P=10MPa and U_G =0.138cm.s^{-1}

3.5 Effect of different liquid and gas phase

The effects of different liquid and gas phase are also evaluated (Fig. 12 and Fig. 13). As shown in Fig. 12, the bubble number in ethanol/water mixture system is much more than that in the water system, which is also presented in Fig. 2 (c). The bubble size distributions are log-normal while the He gas with low density exhibits an observable effect on the bubble distribution curve, which can be attributed to lower momentum force for the low density He gas. Moreover, with the gas velocity increase from 0.138 to 0.276cm.s^{-1}, the bubble size distribution for the four systems (water-N_2, water-He, ethanol/water mixture-N_2 and ethanol/water-He) all become wider and the shifts from small to larger-size bubble, as presented in section 3.1.

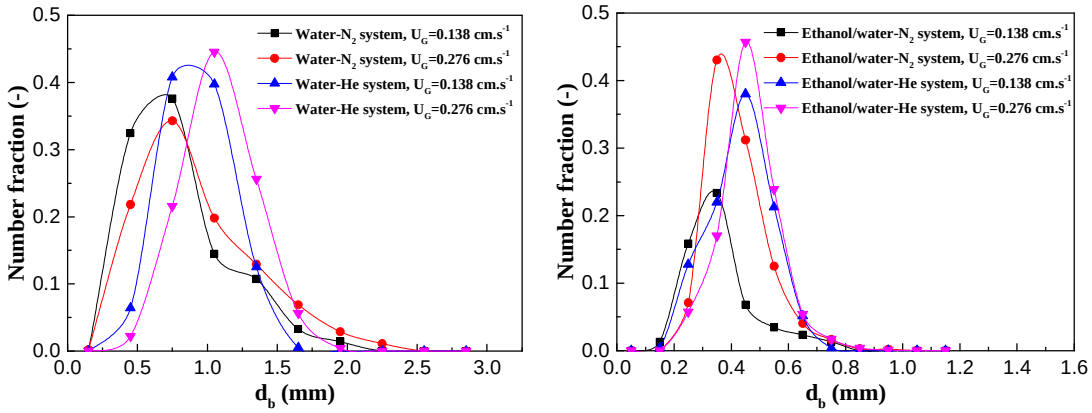

Fig. 12 Bubble number distribution and number fraction distribution under various liquid and gas phase at P=10MPa, T=373K, U_L =0.022cm.s^{-1} and U_G =0.138-0.276cm.s^{-1}

It is observed on Fig. 13 that the mean Sauter diameter, gas holdup and interfacial area are slightly affected by the type of gas employed, but significantly affected by the liquid phase, in agreement with Kanaris et al. (2018) (Kanaris et al., 2018). The Sauter mean diameters of He in water and ethanol/water mixture are generally slight higher than those of N_2 under similar operating conditions (Fig. 13), which is in agreement with literature findings (Behkish et al., 2007). This behaviour may be due to the lower density of He than N_2 under

the same operating conditions shown in Table 2: He is expected to form larger gas bubbles compared with N_2 (Behkish et al., 2007). It is also shown that the Sauter mean diameter in the system using ethanol/water mixture as liquid phase are much smaller than the system using water as liquid phase. That is because the coalescence of bubbles is strongly influenced by the composition of the liquid phase, which is reduced for the mixture liquids in comparison to pure liquids. The liquid mixture can cause coalescence inhibition (Lehr et al., 2002). Pjontek et al. (2014) also found a significant reduction in bubble size with the addition of ethanol in water when comparing to water, which was attributed to the shear stresses acting on the bubbles due to liquid and gas passing through the gas distributor, which increased bubble breakup. Furthermore, as viscosity increases, the drag force increases, leading to the formation of smaller bubbles (Kazakis et al., 2008). Thus in ethanol/water mixture system, coalescence inhibition and shear stresses through the distribution leads to a bubble size reduction.

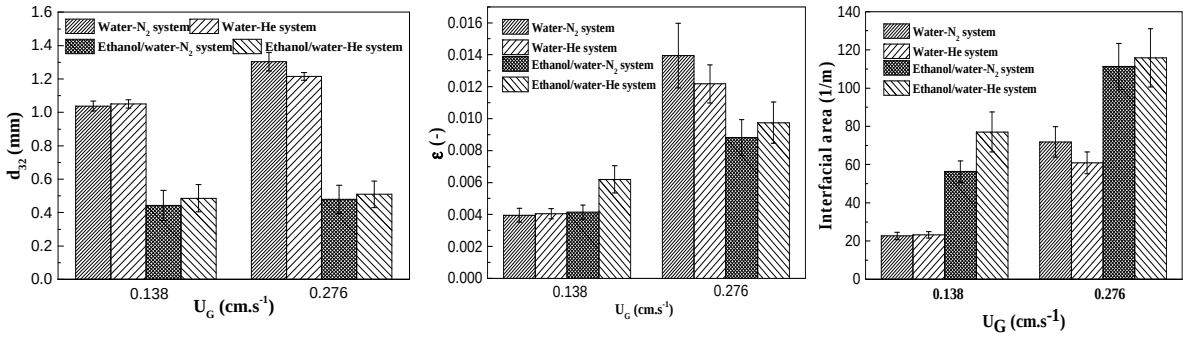

Fig. 13 Bubble mean Sauter diameter (left), gas holdup (middle) and interfacial area (right) under various liquid and gas phase at P=10MPa, T=373K, U_L =0.022cm.s^{-1} and U_G =0.138-0.276cm.s^{-1}

Many researchers observed that with increasing gas density, gas holdup increases, attributing this behaviour to a lower momentum force for the lower density gas in the primary bubble formation at the gas distributor (Hecht Kristin et al., 2015; Kanaris et al., 2018). In this study, the effects of gas phase with different gas density on gas holdup are complex. Fig. 13 shows that in the ethanol/water mixture system, the gas holdup for He is a little bigger than for N_2, while in the water system, the effects of gas phases are different at different superficial gas velocity . The reason for this phenomenon needs to be further studied. At the superficial gas velocity of 0.276cm.s^{-1}, the gas holdup in ethanol/water system with the higher viscosity is smaller than the water system, which is similar to the results in the literature (Besagni et al., 2018; Deng et al., 2010; Ojha and Al-Dahhan, 2018). This behaviour is mainly due to reduced bubble interaction resulting from reduced turbulence and mixing at

higher viscosities (Deng et al., 2010; Ojha and Al-Dahhan, 2018). With the superficial gas velocity at 0.138cm.s^{-1}, the gas holdup are close in the water and in the ethanol/water mixture, which is similar to Fransolet et al. (2005) . Wu et al. (2013) found that with an increase in liquid viscosity, the gas holdup in carboxyl methyl cellulose-water solution first increased and reached a maximum, and then decreased. The reason for the complex effect of liquid phase on gas holdup has been attributed to "dual effect of viscosity" on gas holdup (Besagni et al., 2018). Furthermore, Fig. 13 also shows that the interfacial area for ethanol/water mixture is bigger than water, which is opposite to Ojha et al. (2018) and Wu et al. (2013).

3.6 The correlation for average bubble size and gas holdup

Possible factors affecting the average bubble size and the gas holdup are the column diameter, the diameter of gas inlet orifice, superficial gas velocity, kinematic viscosity, liquid density and surface tension (Akita and Yoshida, 1973). Kanaris et al. (2018) proposed a correlation for predicting the average bubble size and the gas holdup based on dimensionless numbers with general form:

$$\frac{d_{32}}{D} = a_1 \left[We^{a_2} Re^{a_3} Fr^{a_4} \left(\frac{d_p}{D}\right)^{a_5} \right]^{a_6} \tag{8}$$

$$\varepsilon_G = b_1 \left[Eo^{b_2} Ar^{b_3} Fr^{b_4} \left(\frac{d_p}{D}\right)^{b_5} \right]^{b_6} \tag{9}$$

Values of a_1 to a_6, b_1 to b_6 are determined from the experiment data. We, Re, Eo, Ar and Fr are the dimensionless Weber, Reynolds, Eötvos, Archimedes and Froude number respectively (Table 3). The effect of gas velocity can be taken into account by defining *Fr*, *We* and *Re* number and the effect of the physical properties (viscosity, density and surface tension) of the liquid phase can be included in *We*, *Re*, *Ar*, and *Eo* numbers (Maceiras et al., 2010).

Table 3 Dimensionless number for this study

System	*T* (K)	*P* (MPa)	U_G (cm/s)	*We*	*Re*	*Fr*	*Ar*	*Eo*
H_2O-N_2	373	10	0.083	0.000113	28	7.02E-06	31978	16.0
			0.138	0.000311	46	1.94E-05	31978	16.0
			0.193	0.000609	65	3.80E-05	31978	16.0
			0.248	0.001005	83	6.27E-05	31978	16.0
			0.276	0.001245	93	7.77E-05	31978	16.0
	373	15	0.083	0.000113	28	7.02E-06	31961	16.1
			0.138	0.000312	46	1.94E-05	31961	16.1
			0.193	0.000610	65	3.80E-05	31961	16.1
			0.248	0.001007	83	6.27E-05	31961	16.1
			0.276	0.001248	93	7.77E-05	31961	16.1

			0.083	0.000313	27	7.02E-06	31944	16.1
			0.138	0.000313	46	1.94E-05	31944	16.1
	373	20	0.193	0.000611	65	3.80E-05	31944	16.1
			0.248	0.001010	83	6.27E-05	31944	16.1
			0.276	0.001250	92	7.77E-05	31944	16.1
	423	10	0.138	0.000360	683	1.94E-05	45096	18.6
	473	10	0.138	0.000440	88	1.94E-05	54539	22.7
H_2O-He	373	10	0.138	0.000311	4.7	1.94E-05	31979	16.0
			0.276	0.001245	93	7.77E-05	31979	16.0
Ethanol/H_2O-N_2	373	10	0.138	0.00485	24	1.94E-05	13870	25.0
			0.276	0.001938	49	7.77E-05	13870	25.0
Ethanol/H_2O-He	373	10	0.138	0.000485	24	1.94E-05	13870	25.0
			0.276	0.001938	49	7.77E-05	13870	25.0

In this study, the values of the constants a_1-a_6 and b_1-b_6 have been adjusted through changing one parameter with fixing other parameters in order to find the optimal curves. The new correlation Sauter mean diameter and gas holdup are formulated and compared with Kanaris et al. (2018) which is shown in Table 4.

Table 4 Comparison of Sauter mean diameter and gas holdup correlation between Kanaris et al. (2018) and this study

Authors	Diameter correlation	Gas holdup correlation
(Kanaris et al., 2018)	$\frac{d_{32}}{D} = 0.9\left[We^{0.95}Re^{0.40}Fr^{0.47}\left(\frac{d_p}{D}\right)^{0.55}\right]^{0.51}$	$\varepsilon_G = 0.020\left[Eo^{3.5}Ar^{0.015}Fr^{0.300}\left(\frac{d_p}{D}\right)^{1.10}\right]^{2.62}$
In this study	$\frac{d_{32}}{D} = 0.35\left[We^{0.95}Re^{0.40}Fr^{0.47}\left(\frac{d_p}{D}\right)^{0.55}\right]^{0.09}$	$\varepsilon_G = 0.13\left[Eo^{0.64}Ar^{0.85}Fr^{1.77}\left(\frac{d_p}{D}\right)^{0.02}\right]^{0.36}$

Table 4 showed that the exponents (a_2- a_5) of *We*, *Re*, *Fr* and d_p/D for Sauter diameter correlation in this study is the same with Kanaris et al (2018), while $a_1$and a_6 are different. b_1-b_6 for gas holdup correlation in this research are all different with Kanaris et al (2018), which may be due to the different operation conditions between this study with Kanaris et al. (2018). The correlations for Sauter mean diameter and gas holdup in this study are plotted in Fig. 14. The data are in good agreement (±15% for Sauter mean diameter and ±20% for gas holdup) with the corresponding experimental data. Thus, the two correlations are suitable for predicting the bubble average diameter and gas holdup for the bubble column under the WAO operation.

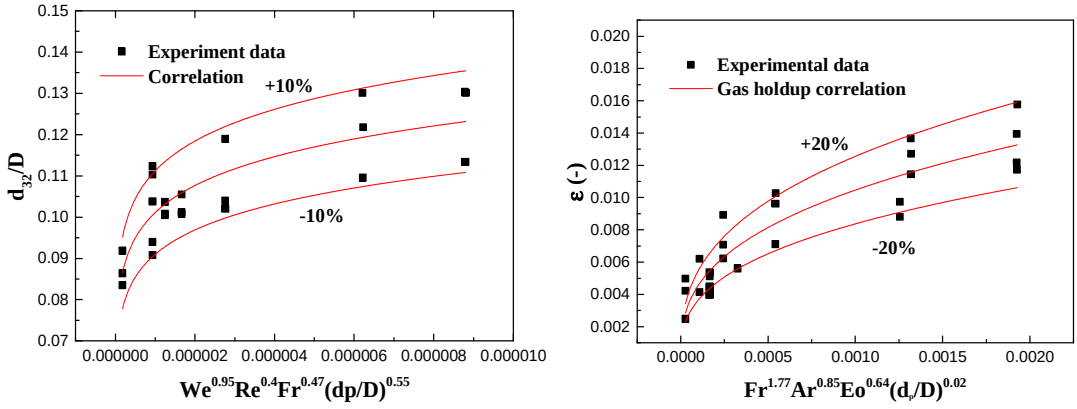

Fig. 14 Comparison of the Sauter mean diameter (left) and gas holdup (right) prediction with experimental data

4 Conclusion

The bubble size distribution, the Sauter mean diameter, the gas holdup and the interfacial area were determined in a bubble column under wet air oxidation conditions with a wide range of gas and liquid superficial velocities, pressure, temperature and different liquid and gas phases. With the increase of superficial gas velocity, the bubble size distribution shifted from small-to- larger size bubble and the Sauter mean diameter, the gas holdup and the interfacial area generally increased due to the increase of coalescence with superficial gas velocity. The bubble size enhanced with the increasing height from the bottom to the top of the column due to coalescence. The effect of superficial liquid velocity on bubble characteristics was not significant. Increasing pressure and temperature resulted in bubble size distribution shifting from larger-to-smaller size bubble. The effect of pressure on the Sauter mean diameter was complex to determine. A marginal decrease in the Sauter mean diameter was found with the increase of temperature. Pressure and temperature slightly affected the gas holdup and the interfacial area. Moreover, bubble characteristics were not considerably affected by the type of the gas phase, but mainly influenced by the liquid phase. Parameters for Kanaris correlation(ref) were given for the prediction of the bubble mean Sauter diameter and gas holdup for the bubble column under high pressure and high temperature in subcritical water conditions. For a unique set of parameters, this correlation was in good agreement with all experimental data (10% for diameter, 20% for gas hold-up). The correlations may be recommended to scale-up the system for gas liquid contactors working at high pressure and temperature, as WAO for instance.

Acknowledge

This work was partly supported by the Chinese Scholarship Council. Authors are grateful to Jean-Paul Nisteron for helpful assistance on the experimental work.

References

Akita, K., Yoshida, F., 1974. Bubble size, interfacial area, and liquid-phase mass transfer coefficient in bubble columns. Ind. Eng. Chem. Process Des. Dev. 13, 84–91.

Akita, K., Yoshida, F., 1973. Gas Holdup and Volumetric Mass Transfer Coefficient in Bubble Columns. Effects of Liquid Properties. Ind. Eng. Chem. Process Des. Dev. 12, 76–80. https://doi.org/10.1021/i260045a015

Barge, A.S., Vaidya, P.D., 2018. Wet air oxidation of cresylic spent caustic – A model compound study over graphene oxide (GO) and ruthenium/GO catalysts. J. Environ. Manage. 212, 479–489. https://doi.org/10.1016/j.jenvman.2018.01.066

Baz-Rodríguez, S.A., Botello-Alvarez, J.E., Estrada-Baltazar, A., Vilchiz-Bravo, L.E., Padilla-Medina, J.A., Miranda-López, R., 2014. Effect of electrolytes in aqueous solutions on oxygen transfer in gas–liquid bubble columns. Chem. Eng. Res. Des. 92, 2352–2360. https://doi.org/10.1016/j.cherd.2014.02.023

Behkish, A., Lemoine, R., Sehabiague, L., Oukaci, R., Morsi, B.I., 2007. Gas holdup and bubble size behavior in a large-scale slurry bubble column reactor operating with an organic liquid under elevated pressures and temperatures. Chem. Eng. J. 128, 69–84. https://doi.org/10.1016/j.cej.2006.10.016

Besagni, G., Gallazzini, L., Inzoli, F., 2018. Effect of gas sparger design on bubble column hydrodynamics using pure and binary liquid phases. Chem. Eng. Sci. 176, 116–126. https://doi.org/10.1016/j.ces.2017.10.036

Chaumat, H., Billet-Duquenne, A.M., Augier, F., Mathieu, C., Delmas, H., 2005. Mass transfer in bubble column for industrial conditions—effects of organic medium, gas and liquid flow rates and column design. Chem. Eng. Sci., 7th International Conference on Gas-Liquid and Gas-Liquid-Solid Reactor Engineering 60, 5930–5936. https://doi.org/10.1016/j.ces.2005.04.026

Chilekar, V.P., 2007. Hydrodynamics and mass transfer in slurry bubble columns: Scale and pressure effects. Citeseer.

Chilekar, V.P., van der Schaaf, J., Kuster, B.F.M., Tinge, J.T., Schouten, J.C., 2010. Influence of elevated pressure and particle lyophobicity on hydrodynamics and gas–liquid mass transfer in slurry bubble columns. AIChE J. 56, 584–596. https://doi.org/10.1002/aic.11987

Clark, K.N., 1990. The effect of high pressure and temperature on phase distributions in a bubble column. Chem. Eng. Sci. 45, 2301–2307.

Deckwer, W.-D., Louisi, Y., Zaidi, A., Ralek, M., 1980. Hydrodynamic Properties of the Fischer-Tropsch Slurry Process. Ind. Eng. Chem. Process Des. Dev. 19, 699–708. https://doi.org/10.1021/i260076a032

Deng, Z., Wang, T., Zhang, N., Wang, Z., 2010. Gas holdup, bubble behavior and mass transfer in a 5m high internal-loop airlift reactor with non-Newtonian fluid. Chem. Eng. J. 160, 729–737. https://doi.org/10.1016/j.cej.2010.03.078

Fransolet, E., Crine, M., Marchot, P., Toye, D., 2005. Analysis of gas holdup in bubble columns with non-Newtonian fluid using electrical resistance tomography and dynamic gas disengagement technique. Chem. Eng. Sci., 7th International Conference on Gas-Liquid and Gas-Liquid-Solid Reactor Engineering 60, 6118–6123. https://doi.org/10.1016/j.ces.2005.03.046

Grover, G.S., Rode, C.V., Chaudhari, R.V., 1986. Effect of temperature on flow regimes and gas hold-up in a bubble column. Can. J. Chem. Eng. 64, 501–504. https://doi.org/10.1002/cjce.5450640321

Hashemi, S., Macchi, A., Servio, P., 2009. Gas–liquid mass transfer in a slurry bubble column operated at gas hydrate forming conditions. Chem. Eng. Sci. 64, 3709–3716. https://doi.org/10.1016/j.ces.2009.05.023

Hecht Kristin, Bey Oliver, Ettmüller Jürgen, Graefen Patrick, Friehmelt Rainer, Nilles Michael, 2015. Effect of Gas Density on Gas Holdup in Bubble Columns. Chem. Ing. Tech. 87, 762–772. https://doi.org/10.1002/cite.201500010

Inga, J.R., Morsi, B.I., 1999. Effect of Operating Variables on the Gas Holdup in a Large-Scale Slurry Bubble Column Reactor Operating with an Organic Liquid Mixture. Ind. Eng. Chem. Res. 38, 928–937. https://doi.org/10.1021/ie980384q

Jin, H., Yang, S., He, G., Liu, D., Tong, Z., Zhu, J., 2014. Gas–Liquid Mass Transfer Characteristics in a Gas–Liquid–Solid Bubble Column under Elevated Pressure and Temperature. Chin. J. Chem. Eng. 22, 955–961. https://doi.org/10.1016/j.cjche.2014.06.019

Kanaris, A.G., Pavlidis, T.I., Chatzidafni, A.P., Mouza, A.A., 2018. On the design of bubble columns equipped with a fine pore sparger: Effect of gas properties. Gas 2, 2.

Kawase, Y., Umeno, S., Kumagai, T., 1992. The prediction of gas hold-up in bubble column reactors: Newtonian and non-newtonian fluids. Chem. Eng. J. 50, 1–7. https://doi.org/10.1016/0300-9467(92)80001-Q

Kazakis, N.A., Mouza, A.A., Paras, S.V., 2008. Experimental study of bubble formation at metal porous spargers: Effect of liquid properties and sparger characteristics on the initial bubble size distribution - ScienceDirect. Chem. Eng. J. 137, 265–281.

Kumar, S., Munshi, P., Khanna, A., 2012. High Pressure Experiments and Simulations in Cocurrent Bubble Columns. Procedia Eng., CHISA 2012 42, 842–853. https://doi.org/10.1016/j.proeng.2012.07.477

Lau, R., Peng, W., Velazquez-Vargas, L.G., Yang, G.Q., Fan, L.-S., 2004. Gas−Liquid Mass Transfer in High-Pressure Bubble Columns. Ind. Eng. Chem. Res. 43, 1302–1311. https://doi.org/10.1021/ie030416w

Lehr, F., Millies, M., Mewes, D., 2002. Bubble-Size distributions and flow fields in bubble columns. AIChE J. 48, 2426–2443.

Leonard, C., Ferrasse, J.-H., Boutin, O., Lefevre, S., Viand, A., 2015. Bubble column reactors for high pressures and high temperatures operation. Chem. Eng. Res. Des. 100, 391–421. https://doi.org/10.1016/j.cherd.2015.05.013

Leonard, C., Ferrasse, J.-H., Boutin, O., Lefevre, S., Viand, A., Measurements and correlations for gas liquid surface tension at high pressure and high temperature, AIChE Journal, https://doi.org/10.1002/aic.16216

Li, X., Jaworski, A.J., Mao, X., 2018. Bubble size and bubble rise velocity estimation by means of electrical capacitance tomography within gas-solids fluidized beds. Measurement 117, 226–240. https://doi.org/10.1016/j.measurement.2017.12.017

Lin, T.-J., Tsuchiya, K., Fan, L.-S., 1998. Bubble flow characteristics in bubble columns at elevated pressure and temperature. AIChE J. 44, 545–560.

Luo, X., Lee, D.J., Lau, R., Yang, G., Fan, L.-S., 1999. Maximum stable bubble size and gas holdup in high-pressure slurry bubble columns. AIChE J. 45, 665–680.

Maalej, S., Benadda, B., Otterbein, M., 2003. Interfacial area and volumetric mass transfer coefficient in a bubble reactor at elevated pressures. Chem. Eng. Sci. 58, 2365–2376. https://doi.org/10.1016/S0009-2509(03)00085-X

Maceiras, R., Álvarez, E., Cancela, M.A., 2010. Experimental interfacial area measurements in a bubble column. Chem. Eng. J. 163, 331–336. https://doi.org/10.1016/j.cej.2010.08.011

Majumder, S.K., Kundu, G., Mukherjee, D., 2006. Bubble size distribution and gas–liquid interfacial area in a modified downflow bubble column. Chem. Eng. J. 122, 1–10. https://doi.org/10.1016/j.cej.2006.04.007

Mohagheghian, S., Elbing, B.R., 2018. Characterization of Bubble Size Distributions within a Bubble Column. Fluids 3, 13. https://doi.org/10.3390/fluids3010013

Mouza, A.A., Dalakoglou, G.K., Paras, S.V., 2005. Effect of liquid properties on the performance of bubble column reactors with fine pore spargers. Chem. Eng. Sci. 60, 1465–1475. https://doi.org/10.1016/j.ces.2004.10.013

Ojha, A., Al-Dahhan, M., 2018. Local gas holdup and bubble dynamics investigation during microalgae culturing in a split airlift photobioreactor. Chem. Eng. Sci. 175, 185–198. https://doi.org/10.1016/j.ces.2017.08.026

Oyevaar, M.H., Bos, R., Westerterp, K.R., 1991. Interfacial areas and gas hold-ups in gas—liquid contactors at elevated pressures from 0.1 to 8.0 MPa. Chem. Eng. Sci. 46, 1217–1231. https://doi.org/10.1016/0009-2509(91)85050-8

Pjontek, D., Parisien, V., Macchi, A., 2014. Bubble characteristics measured using a monofibre optical probe in a bubble column and freeboard region under high gas holdup conditions. Chem. Eng. Sci. 111, 153–169. https://doi.org/10.1016/j.ces.2014.02.024

Pohorecki, R., Moniuk, W., Zdrójkowski, A., 1999. Hydrodynamics of a bubble column under elevated pressure. Chem. Eng. Sci. 54, 5187–5193.

Pohorecki, R., Moniuk, W., Zdrójkowski, A., Bielski, P., 2001. Hydrodynamics of a pilot plant bubble column under elevated temperature and pressure. Chem. Eng. Sci., 16th International Conference on Chemical Reactor Engineering 56, 1167–1174. https://doi.org/10.1016/S0009-2509(00)00336-5

Ramezani, M., Mostoufi, N., Mehrnia, M.R., 2012. Improved Modeling of Bubble Column Reactors by Considering the Bubble Size Distribution. Ind. Eng. Chem. Res. 51, 5705–5714. https://doi.org/10.1021/ie202914s

Schäfer, R., Merten, C., Eigenberger, G., 2002. Bubble size distributions in a bubble column reactor under industrial conditions. Exp. Therm. Fluid Sci. 26, 595–604.

Sehabiague, L., Lemoine, R., Behkish, A., Heintz, Y.J., Morsi, B.I., 2005. Hydrodynamic and Mass Transfer Parameters in a Slurry Bubble Column Reactor Operating under Fischer-Tropsch Conditions. Presented at the Conference Proceedings of AIChE Annual Meeting, Cincinnati, USA, p. 9918.

Shahrouz Mohagheghian, Brian Elbing, 2018. Characterization of Bubble Size Distributions within a Bubble Column. Fluids 3, 13. https://doi.org/10.3390/fluids3010013

Stegeman, D., Knop, P.A., Wijnands, A.J.G., Westerterp*, K.R., 1996. Interfacial Area and Gas Holdup in a Bubble Column Reactor at Elevated Pressures - Industrial & Engineering Chemistry Research (ACS Publications). Ind. Eng. Chem. Res. 35, 3842–3847.

Sturges, H.A., 1926. The Choice of a Class Interval. J. Am. Stat. Assoc. 21, 65–66. https://doi.org/10.1080/01621459.1926.10502161

Tang, C., Heindel, T.J., 2006. Estimating gas holdup via pressure difference measurements in a cocurrent bubble column. Int. J. Multiph. Flow 32, 850–863. https://doi.org/10.1016/j.ijmultiphaseflow.2006.02.008

Thermophysical properties of fluid systems [WWW Document], n.d. URL http://webbook.nist.gov/chemistry/fluid/ (accessed 3.1.18).

Therning, P., Rasmuson, A., 2001. Liquid dispersion, gas holdup and frictional pressure drop in a packed bubble column at elevated pressures. Chem. Eng. J. 81, 331–335. https://doi.org/10.1016/S1385-8947(00)00222-9

Urseanu, M.I., Guit, R.P.M., Stankiewicz, A., van Kranenburg, G., Lommen, J.H.G.M., 2003. Influence of operating pressure on the gas hold-up in bubble columns for high viscous media. Chem. Eng. Sci., 17th International Symposium of Chemical Reaction Engineering (IS CRE 17) 58, 697–704. https://doi.org/10.1016/S0009-2509(02)00597-3

Wilkinson, P.M., Haringa, H., Van Dierendonck, L.L., 1994. Mass transfer and bubble size in a bubble column under pressure. Chem. Eng. Sci. 49, 1417–1427. https://doi.org/10.1016/0009-2509(93)E0022-5

Wilkinson, P.M., Spek, A.P., Dierendonck, V., L, L., 1992. Design parameters estimation for scale□ up of high□pressure bubble columns. AIChE J. 38, 544–554. https://doi.org/10.1002/aic.690380408

Wilkinson, P.M., Spek, A.P., van Dierendonck, L.L., 1991. Design parameters estimation for scale-up of high-pressure bubble columns. AIChE J. 38, 544–554. https://doi.org/10.1002/aic.690380408

Yang, W., Wang, J., Jin, Y., 2001. Mass Transfer Characteristics of Syngas Components in Slurry System at Industrial Conditions. Chem. Eng. Technol. 24, 651–657. https://doi.org/10.1002/1521-4125(200106)24:6<651::AID-CEAT651>3.0.CO;2-X